AAPS PharmSciTech, Vol. 15, No. 2, April 2014 (© 2013)
DOI: 10.1208/s12249-013-0056-9

Research Article

Lipid Effects on Expulsion Rate of Amphotericin B from Solid Lipid Nanoparticles

See Wei Tan[1] and Nashiru Billa[1,2]

Received 31 July 2013; accepted 15 November 2013; published online 7 December 2013

Abstract. We aimed to investigate the effects that natural lipids, theobroma oil (TO) and beeswax (BW), might have on the physical properties of formulated nanoparticles and also the degree of expulsion of encapsulated amphotericin B (AmB) from the nanoparticles during storage. Lecithin and sodium cholate were used as emulsifiers whilst oleic acid (OA) was used to study the influence of the state of orderliness/disorderliness within the matrices of the nanoparticles on the degree of AmB expulsion during storage. BW was found to effect larger z-average diameter compared with TO. Lecithin was found to augment the stability of the nanoparticles imparted by BW and TO during storage. An encapsulation efficiency (%EE) of 59% was recorded when TO was the sole lipid as against 42% from BW. In combination however, the %EE dropped to 39%. When used as sole lipid, TO or BW formed nanoparticles with comparatively higher enthalpies, 21.1 and 23.3 J/g respectively, which subsequently caused significantly higher degree of AmB expulsion, 81 and 83% respectively, whilst only 11.8% was expelled from a binary TO/BW mixture. A tertiary TO/BW/OA mixture registered the lowest enthalpy at 8.07 J/g and expelled 12.6% of AmB but encapsulated only 22% of AmB. In conclusion, nanoparticles made from equal concentrations of TO and BW produced the most desirable properties and worthy of further investigations.

KEY WORDS: amphotericin B; beeswax; expulsion; lipid nanoparticles; theobroma oil.

INTRODUCTION

Amphotericin B (AmB), a non-aromatic polyene antifungal antibiotic can be isolated from fermented cultures of *Streptomyces nodosus* (1) and has remained as the "gold standard" for treating life-threatening systemic fungal infections for the past 30 years (2). However, its usefulness is partly limited due to the poor absorption from the gastrointestinal tract. Therefore, AmB is administered exclusively parenterally. The constraints to delivering drugs parenterally are well documented, and in addition, side-effects due to AmB are exacerbated when it is delivered parenterally. Some of the side effects due to AmB can be potentially minimised when it is administered orally. Therefore, the ultimate aim would be to enhance the bioavailability of AmB, whilst addressing the side effects associated with parenteral delivery. Recent studies indicate that this is achievable by formulating AmB in lipid nanoparticulate delivery systems (3–5). Different lipids behave differently in aqueous environment (6) and have different crystallinity profiles and, hence, capacities for accommodating foreign molecules. A prerequisite for enhanced drug accommodation within the matrix of lipid nanoparticles matrices is large distances between fatty acid chains constituting the lipids and general imperfections within the lipid crystal lattices that can accommodate drug moieties. To achieve high degree of imperfection within the lipid crystal, spatially incompatible lipids (glycerides composed of very different fatty acids *e.g.* in length of carbon chain, or mixture of saturated and unsaturated acids) have been used. One of the major constraints to formulating lipid nanoformulation is that the payload is prone to expulsion during storage. An advantage of imperfect lattices is that drug expulsion during storage is checked (5). In the present study, AmB-containing lipid nanoparticles with submicronic size were fabricated using natural lipids: beeswax (BW), theobroma oil (TO) and oleic acid (OA). TO and BW are solid lipids at room temperature (25°C). BW is obtained from honeybee combs and is relatively stable. TO is obtained from the plant *Theobroma cocao* but polymorphic transformations of TO are well recognized (7). Nevertheless, both lipids are biocompatible. Attama *et al.* (8) has established that lipid cores obtained from TO/BW matrices consist of small fractions of mixed crystals favourable for improved drug loading. OA is a mono-unsaturated fatty acid from plant and animal sources and was employed in the present study due to its physical compatibility with TO/BW composite. Being liquid at room temperature, OA is likely to disrupt the crystalline lattices of TO/BW composites (9). The aim of the present study was to formulate lipid nanoparticulate delivery system using the above lipids and study their effects on AmB encapsulation and expulsion during storage.

MATERIALS AND METHODS

Materials

Beeswax, sodium cholate (SC) and amphotericin B (AmB) were purchased from Sigma (Sigma-Aldrich Co. LLC., St Louis, Missouri, USA). Lecithin was obtained from Fluka whilst ethyl

[1] School of Pharmacy, The University of Nottingham, Malaysia Campus, 43500, Semenyih, Selangor, Malaysia.
[2] To whom correspondence should be addressed. (e-mail: Nashiru.Billa@nottingham.edu.my)

acetate and OA were obtained from R&M (Reichle & De-Massari AG, Wetzikon, Switzerland). TO was obtained from Kondima (Kondima Engelhardt GmbH & Co. KG, Karlsruhe Stösserstraße, Germany). Methanol, chloroform and all other reagents were analytical-grade and purchased from R&M (Reichle & De-Massari AG, Wetzikon, Switzerland).

Formulation of Lipid Nanoparticles

AmB-containing lipid nanoparticles formulated by a solvent diffusion method was carried out as described by Quintanar-Guerrero *et al.* (10), with slight modifications, namely, polymers were replaced with lipids in the present study. Briefly, AmB was first dissolved in a chloroform–methanol (2:1) mixture, along with the lipids (BW, OA and TO) and lecithin (refer to Table I), followed by removal of organic solvents using a Büchi Rotavapor®, model R-200/205. The lipid matrix containing the AmB was then dissolved in 10 ml of ethyl acetate (previously equilibrated with water for 10 min to reach thermodynamic equilibrium) at 70°C. At the same time, 20 ml of the 5% aqueous solution of sodium cholate was heated to the same temperature. Both phases were mixed and then homogenized using a high-speed homogenizer (Ika-Turrax) at 10,000 rpm for 10 min. Then, 80 ml of water at 70°C was added slowly into the mixture with continuous stirring for a further 20 min before being subjected to ultrasonication using a high-intensity ultrasonicator (Vibra Cell, Sonics, USA) at amplitude of 35% with a pulse ratio on/off 2/3 for 20 min. Finally, the organic solvent was evaporated by using Büchi Rotavapor®.

Photon Correlation Spectroscopy Analyses

Photon correlation spectroscopy studies were carried out using Zetasizer Nano ZS (Malvern, UK) equipped with a 4 mW He–Ne laser (633 nm). The parameters measured were polydispersity index (PDI), *z*-average diameter, particle size distribution profile (PDI) and the zeta potential (ζ). In evaluating the particle size, the intensity distribution was used, and hence the *z*-average diameter is an intensity mean diameter, and the PDI describes the width of the particle size distribution. The ζ, which measures the surface charge of the reconstituted nanoparticles, was analysed by the software based on the Henry equation through determining the electrophoretic mobility of the sample. Prior to analysis, each sample was diluted to 0.1% (*w/v*) of lipids with deionized (DI) water. Each analysis was carried out at 25°C and performed in triplicates whilst the data are expressed as mean±standard deviation.

High-Pressure Liquid Chromatography Analyses

The encapsulation of AmB within the lipid nanoparticles was estimated using high-pressure liquid chromatography (HPLC) as follows: The pH of a 1 mL aliquot of the prepared formulation was adjusted to 1.2 with a few drops of 0.1 M hydrochloric acid to precipitate the nanoparticles, followed by centrifugation at 11,000 rpm for 45 min at 16°C. The supernatant was then decanted, and 425 μl of dimethyl sulfoxide (DMSO) with 100 μl of 0.01% 1-amino-4-nitronaphthalene (internal standard) was added to the pellet at the bottom of the tube, prior to heating to 70°C. A 420-μl aliquot of this solution was added to 750 μl of DI water, vortex-mixed and then centrifuged at 11,000 rpm for 10 min. The amount of AmB was determined by injecting 20 μl of the supernatant onto the HPLC system (PerkinElmer, Shelton, Connecticut, USA) equipped with a 15 cm×4.6 mm reversed-phase C-18 column (Apex ODS, Grace, USA) filled with a 5 μm particle size stationary phase. Detection of AmB in the sample was by ultraviolet at 405 nm. The mobile phase comprised of 70% 2.5 mM EDTA and 30% acetonitrile. The method was validated with regard to linearity of responses to concentration, and the correlation coefficient was found to be >0.9. Analyses were performed in triplicates and expressed as mean values± standard deviation. AmB content was determined by calculating the peak–height ratio of AmB to the internal standard and comparing these to the same from the standard curve.

The percentage efficiency (%EE) of AmB encapsulation within the lipid nanoparticles was calculated using the following relationship:

$$\%EE = \frac{\text{Amount of drug in precipitate}}{\text{Amount of drug added}} \times 100 \qquad (2.1)$$

The amount of drug in the precipitate (amount of AmB encapsulated) was obtained by multiplying the amount of AmB detected by HPLC with the dilution factor when

Table I. Lipid Nanoparticle Suspensions Prepared with Different Lipid Combinations by Solvent Diffusion

	20 ml of aqueous sodium cholate solution	Lecithin	Lipid matrix (Total 400 mg)			AmB	Water
			Solid lipid (% *w/w*)		Liquid lipid (% *w/w*)		
Formulation	(% *w/w*)	(% *w/w* of total lipid)	TO	BW	OA	(mg)	(ml)
SDL1	5.0	30.0	100.0	–	–	10.0	80.0
SDL2	5.0	30.0	–	100.0	–	10.0	80.0
SDL3	5.0	30.0	50.0	50.0	–	10.0	80.0
SDL4	5.0	30.0	33.3	33.3	33.3	10.0	80.0
SDL5	5.0	–	–	100.0	–	10.0	80.0

AmB amphotericin B, *TO* theobroma oil, *BW* beeswax, *OA* oleic acid

DMSO, 1-amino-4-nitronaphthalene and DI water were added.

The difference between %EE at time of preparation ($\%EE_0$) and after 1 month of storage ($\%EE_1$) at ambient temperature (25°C) was used to estimate the degree of AmB expulsion from the nanoparticles during that period:

$$\text{Degree of AmB expulsion } (\%) = \frac{\%EE_0 - \%EE_1}{\%EE_0} \times 100 \quad (2.2)$$

Each analysis was performed in triplicates, and the data are expressed as mean±standard deviation.

Differential Scanning Calorimetric Analyses

Differential scanning calorimetric analyses were performed using a Mettler Toledo DSC 823E, equipped with STARe software version 9.01. The melting endotherms were used to calculate the enthalpy at melt for the lipid nanoparticles, which in turn gave an indication of the extent of order within each system. Approximately 5 mg of sample was placed on standard aluminum pans and heated at a rate of 10°C/min from −20 to 80°C. Analysis was performed under a gentle nitrogen purge using an empty pan as reference. The melting enthalpy of each sample was calculated using the STARe® software *via* integration of the melting peaks. Each analysis was performed in triplicates, and the data are expressed as mean±standard deviation.

Field Emission Scanning Electron Microscopy (FESEM) and Scanning Transmission Electron Microscopy (STEM) Analyses

Morphology of the lipid nanoparticles were examined using a Carl Zeiss Supra 55VP-30-86 FE-SEM in high vacuum mode. Prior to analysis, samples were diluted with DI water (1:100), mounted on the stage and then air-dried. They were then osmium tetraoxide-fixed before viewing under field emission at 4.0 kV. Samples for STEM imaging were similarly prepared without fixation and observed under scanning transmission at 30 kV, using a Supra 40VP-31-31 SEM. Stem images gave some insights on the internal conformation within the nanoparticles.

Statistical Analyses

Statistical analyses were performed using PASW Statistic software version 18.0. The physical properties between formulations were compared where appropriate, using a one-way analysis of variance procedure together with Tukey's *post hoc* test. The physical parameters of lipid nanoparticles before and after storage were compared using paired Student's *t*test. In all cases, statistical significant difference was indicated when $P \leq 0.01$.

RESULTS AND DISCUSSION

Effects of Lipids on *Z*-Average

Lipids have profound effects on the physical properties and functionality of the nanoparticles they form. In the present study, BW, TO and OA were used at various ratios in the formulation of the nanoparticles and their effects on the physical properties of the nanoparticles, including *z*-average, surface charge and degree of AmB expulsion from the nanoparticles during storage will be discussed in depth. The formulations studied are presented in Table I and were prepared as described in Section "Formulation of Lipid Nanoparticles."

The size parameters (*z*-average diameter and PDI) of the lipid nanoparticles were found to be affected by the viscosity of the lipid forming the matrices and the presence or absence of lecithin. Reference viscosity values of BW, TO and OA are >1,000.0 cSt (11), 15.8 cSt (12) and 8.0 cSt (13), respectively, at 70°C. From Fig. 1, it is observed that the freshly prepared nanoformulation SDL2, formulated with BW as the sole lipid, had a significantly higher ($p \leq 0.01$) *z*-average diameter (265.0±6.57 nm) compared with freshly prepared nanoformulation SDL1 (209.6±0.57 nm) formulated with TO as the sole lipid. This difference was obviously due to the higher viscosity of BW when compared with that of TO at the processing temperature of 70°C. During formulation at the same shear force, the higher viscosity component offers more resistance to disperse and therefore retains a comparatively larger size distribution. Furthermore, SDL1 recorded a higher ($p \leq 0.01$) PDI value (0.187±0.02) compared with SDL2 (0.119±0.02), and this can be attributed to the fact that smaller-sized particles have a higher rate of Brownian motion and hence collisions (5). Some of those collisions do result in aggregation of the particles into larger ones which manifests in the formation of dispersions with a wider scatter of sizes (PDI values), as observed in SDL1 when compared with SDL2.

The freshly prepared nanoformulation in which TO and BW were used at identical weight ratios (SDL3), produced nanoparticles whose *z*-average remained essentially unchanged (269.3±5.03 nm) when compared with nanoparticles formulated with BW as the sole lipid (SDL2). Furthermore, there was a slight increase in the PDI value (0.179±0.01) of SDL3. When all three lipids were used to formulate the nanoparticles at equal proportions (SDL4), a *z*-average of 245.3±8.14 nm and PDI of 0.137±0.01 were recorded, both of which are significantly ($p \leq 0.01$) different from the same parameters in SDL2. On the other hand, when BW was used as the sole lipid but in the absence of lecithin (SDL5), we observed a significant increase in both the *z*-average diameter (378.0±14.00 nm) and PDI (0.248±0.02) in the freshly prepared sample. Clearly, the effects of viscosity imparted by the lipids are crucial to the *z*-average diameter of formed nanoparticles. Furthermore, the presence of surfactants is also necessary in the formation of nanoparticles with smaller *z*-averages. The above data confirm what is already known of lipids on *z*-average but also suggests that the effect of the higher melting point component on *z*-average is only marginally reduced in the presence of lower melting point lipids. A summary of measured parameters is presented in Table II.

Effects of Storage on Z-Average of Nanoformulations

During 1 month storage of the nanoformulations, there were transient decreases in the *z*-averages of nanoformulations SDL1, SDL2 and SDL3, albeit insignificantly different from the fresh formulations (Fig. 1). Conversely, there were increases in the *z*-averages of SDL4 and SDL5. These data suggest that the

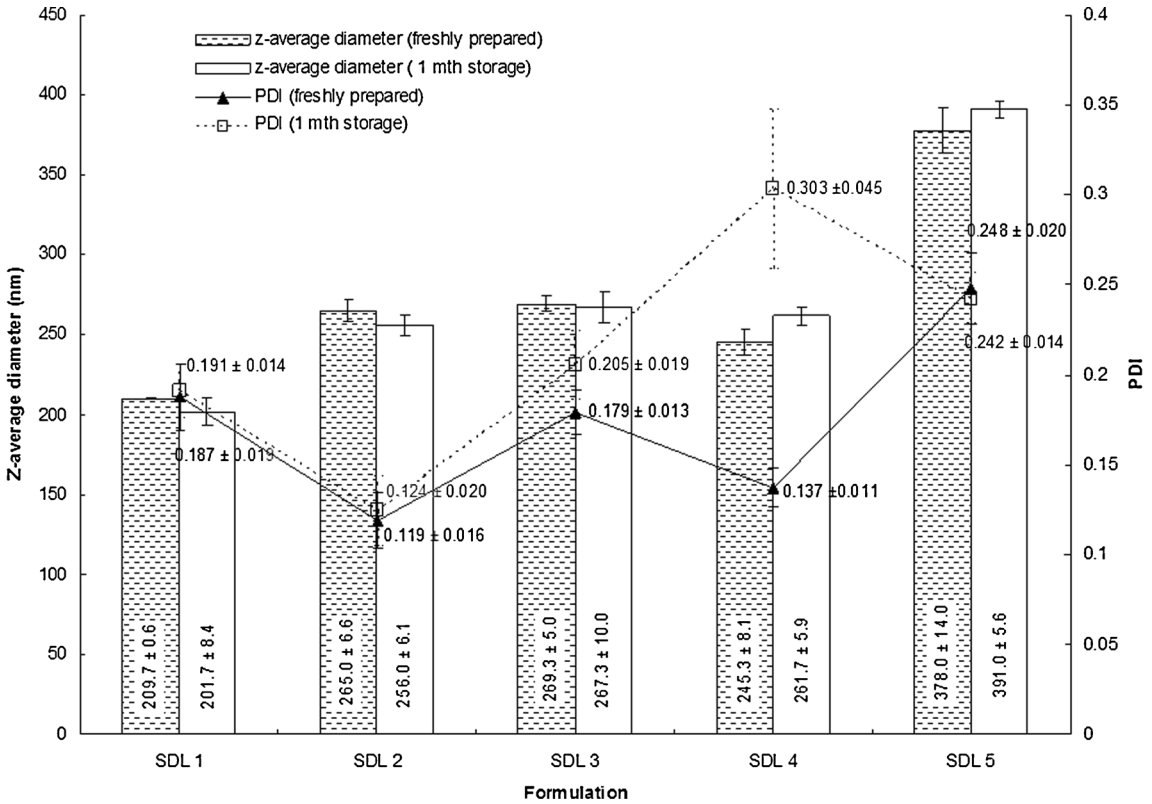

Fig. 1. *Z*-average diameters and polydispersity indices (PDIs) of freshly formulated lipid nanoparticle suspensions and after 1 month of storage ($n=3$)

solid lipids used in the present study (BW and TO) and present in SDL1, SDL2, or SDL3 are better capable in retaining the *z*-average of the nanoparticles in the presence of lecithin during storage. On the other hand, when BW was used for formulating the nanoparticles in the absence of lecithin (SDL5), an increase in *z*-average was observed during storage. Therefore, the presence of lecithin was necessary in checking the growth of *z*-average during storage. Finally, the inclusion of OA (liquid at ambient temperature), along with BW and TO in the formulation (SDL4), produced nanoparticles with a slight increase in *z*-average during storage but a significantly high PDI (0.303± 0.04). Therefore, the *z*-average may not be a true reflection due to the wide scatter of size. This wider scatter of sizes observed with SDL4 could in part be the result of expulsion of some OA along with minute quantities of BW or TO, forming tiny fragments.

Zeta Potential (ζ) of Freshly Prepared Nanoformulations

The ζ allows prediction about the stability of colloidal suspensions (14). In general, particle aggregation is less likely to occur for charged particles with values of ζ>± 30 mV due to electrical repulsion (15,16). All the nanoformulations studied (SDL1 through 5) possessed a negative ζ (Fig. 2), which were above −30 mV. The negative charge can be attributed to the charged nature of the lipids. This suggests that the nanoparticles exist as a matrix rather than a core shell. A representative STEM image of nanoparticle (Section "Zeta Potential (ζ) of Freshly Prepared Nanoformulations") adds credence to the above, since the internal structure of the nanoparticle appears to be uniform. From Fig. 2, the measured ζ was found to be higher in SDL1 (−59.1±1.40 mV) compared with SDL2 (−50.7± 0.58 mV) at the significance level of $p \leq 0.01$ (see Table II). This

Table II. Summary of Measured Parameters from Nanoformulations and Bases

Formulation	*z*-average (nm)		ζ (mV)	%EE		Total enthalpy (J/g)
	Fresh	After 1 month		Fresh	After 1 month	
SDL1	209.7±0.6	201.7±8.4	59.1±1.4	59.0±2.4	11.0±1.1	21.1±1.8
SDL2	265.0±6.6	265.0±6.1	50.7±0.6	42.5±1.6	6.9±0.3	23.3±1.6
SDL3	269.3±5.0	267.0±10.0	50.6±1.0	38.7±2.4	30.7±1.3	11.8±2.0
SDL4	245.3±8.1	261.7±5.9	45.3±0.6	22.1±0.2	19.3±1.0	8.0±0.9
SDL5	378±14.0	391.0±5.6	67.8±2.2	53.2±2.6	42.9±1.3	31.3±0.8
Bulk TO	–		–		–	89.6±5.2
Bulk BW	–		–		–	178.3±3.2

EE encapsulation efficiency, *TO* theobroma oil, *BW* beeswax

suggests that there are more charged groups contributed by TO than from BW (both lipids were respectively present at the same concentration; see Table I). TO has a glyceryl backbone in which two of the –OH are replaced with palmitic acid and the other, with oleic acid. The charged aspect of the lipid originates from the reduced oxygen groups of the acids. BW, on the other hand (SDL2), contains triacontayl palmitate as the major component which has fewer ionisable groups. When TO and BW were used at equal concentrations (SDL3), there was no significant difference between the ζ of the nanoformulation when compared with SDL2 made with BW as the sole lipid. It must be added, however, that the concentration of TO in SDL3 was half that in SDL1 which may explain the reduction of ζ in SDL3. Obviously, the two lipids SDL3 contribute to the charge density observed.

When all three lipids were used at a third part by weight of each (SDL4), the ζ was −45.3±0.61 mV, being the lowest in the series. This reduction in ζ was aptly due to the reduced concentration of both TO and BW but also suggest that the charge contribution by OA is minimal. Finally, in SDL 5 the ζ was the highest, at −67.8±2.19 mV (Table II). This formulation mirrors SDL2 except that it was without lecithin. We may conclude that lecithin condenses the negative charge density contributed by lipids. The positive charge on the tertiary nitrogen in the choline group of lecithin is responsible for condensing the negative charge contribution from the lipids.

Encapsulation Efficiency (%EE) of AmB Within Lipid Matrices

The crystalline structure within the lipid nanoparticles is a key factor to determining whether encapsulated drug would be expelled or be retained during storage. Lipid matrices that form ordered crystalline domains would promote drug expulsion during storage. On the other hand, the imperfect lipid structure (lattice defects) could confer more space to accommodate drugs. As a result, the structure of a less ordered arrangement in the lipid nanoparticles is beneficial to the drug loading capacity (17,18). Figure 3 shows the % EE of AmB and the degree of expulsion from the nanosuspensions before and after a month of storage. From the figure, SDL1 nanoformulated with TO as the sole lipid showed higher ($p \leq 0.01$) %EE (59.0±2.43%) compared with nanoformulation SDL2 prepared with BW as the sole lipid (% EE=42.5± 1.57%). This difference can be attributed to the polymorphism exhibited (displaying α, γ, β′ and β metastable crystals) by TO when heated above 36°C (11). These variant crystal forms of TO causes the arrangement within the lipid matrix to become highly disordered upon solidification at room temperature, and ultimately more space is made available to accommodate AmB. On the other hand, BW exhibits little or no polymorphic transitions (8,9); hence, it is less capable in encapsulating AmB compared with TO during the initial stage of production. The capability of BW to encapsulate AmB, however, was due to its typical crystal structure which combines both crystalline and amorphous characteristics. During cooling and solidification of BW, the long chain wax molecules align themselves, forming various sizes of crystallites (at least two types of crystallites are involved in BW) called the crystalline zones (19). Due to the variation in chain lengths of the wax constituents (predominatly triacontanyl palmitate), zones with voids and loose ends are formed at the crystal borders. These zones are called the chain-end defect or rigid amorphous zones. Components which cannot be accommodated well into crystallites, such as shorter chains, branched chains, unsaturated chains and oils, usually fill up the room between the crystallites, creating the so-called mobile amorphous zones (20).

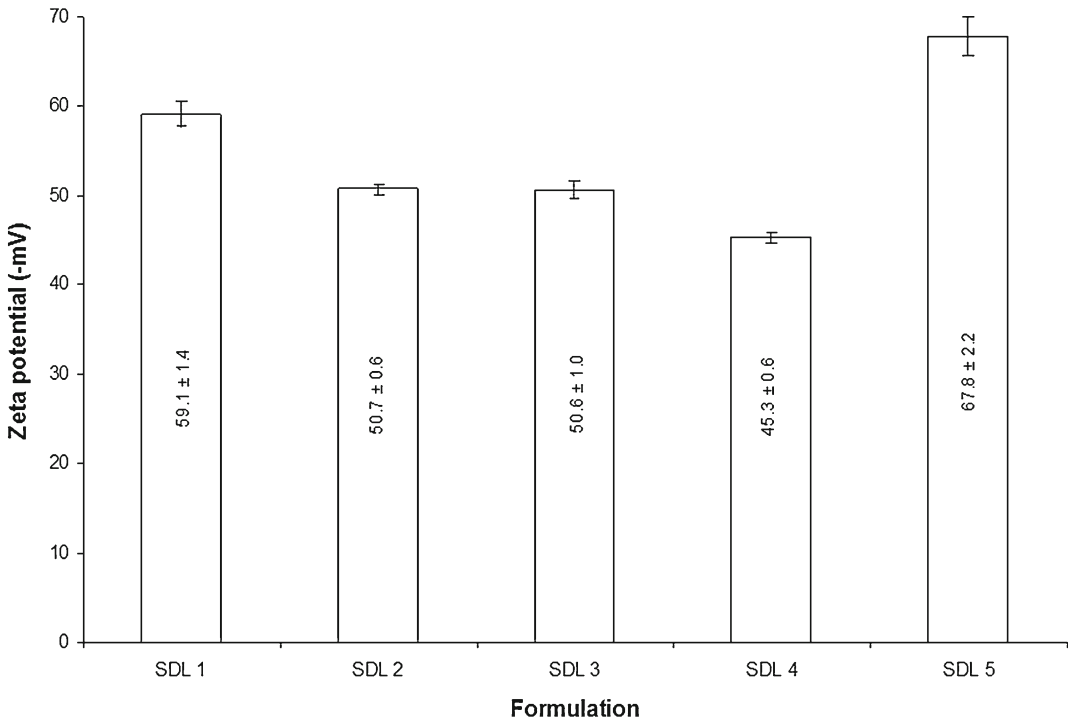

Fig. 2. Zeta potentials of the freshly prepared lipid nanoparticle suspensions (n=3)

Consequently, crystallisation of BW occurs in such a way that is consistent of a network of interlocked wax crystallites with amorphous components immobilising the drug moeities within. Results showed that, when TO and BW were used at equal proportions (SDL3), the %EE (38.7±2.39%) was significantly lower ($p \leq 0.01$) compared with when TO was used alone (SDL1, %EE=58.9±2.43%) (Table II). This suggests that the presence of BW reduces the imperfections caused by the polymorphic transitions within pure TO, hence less drug remains entrapped during solidification. A drastic reduction ($p \leq 0.01$) of %EE (22.1±0.19%) was observed when all three lipids were used in equal portions (SDL4) and can be attributed to the loss of some of the OA during solidification which drains along with any dissolved AmB. This phenomenon of OA leakage is apparent as the lowest AmB expulsion was observed during storage for 1 month. Notwithstanding, the presence of OA contributed to the formation of imperfect domains within the solid TO and BW matrix, but the effect of the expulsion supersedes. The %EE in SDL5 was 53.2± 2.56%, significantly higher than %EE in SDL2 (42.5±1.57%). The two formulations differ in the absence of lecithin in SDL5. This difference in %EE could be attributable to the relatively smaller *z*-average diameter (larger surface area) of SDL2 which promoted leaching of AmB during the formulation process.

Thermal Analyses of Nanoformulations

Melting enthalpy correlates with the presence of impurities or less ordered crystal lattices. For the less ordered or amorphous state crystals, the melting episode of the material does not require or require less energy compared with more perfect crystalline materials where strong lattice forces must be overcome. As a result, higher melting enthalpy values suggest ordered lattice arrangement and *vice versa* (21). In the present study, melting enthalpies of the nanoformulations (after 1 month of production) were determined by integration of the endotherms using linear baseline correction within the range of −20°C to 80°C. Figure 4 shows the DSC thermograms of the melting episodes whilst Fig. 5 shows calculated enthalpies of bulk matrices and nanoformulations. The melting enthalpy of bulk TO was 178.8±3.19 J/g whilst bulk BW displayed an enthalpy of 89.6±5.29 J/g. The melting points were 36.6±0.33°C and at 63.5±1.43°C for TO and BW, respectively (Table II). These DSC thermographic data obtained for bulk TO and BW are in agreement with those reported by other researchers (8,22,23). When both solid lipids were formulated into nanoparticles as sole lipids: SDL1 (TO only) and SDL2 (BW only), the melting points remained unchanged ($p \geq 0.05$) as shown in Fig. 4. However, the melting enthalpy of both nanoformulations (SDL1 and SDL2) decreased drastically ($p \leq 0.01$) when compared, respectively, to the bulk lipids: 21.1±1.35 J/g (SDL1) and 23.3±1.62 J/g (SDL2). Therefore, we may conclude that the lipid matrices within these nanoformulations are less ordered compared with the bulk materials from which they were made. When these lipids (TO and BW) were used at equal proportions (SDL3), we observed two melting peaks at 36.0±0.20 and 62.0±0.46°C with onset temperature of 32.6±0.48 and 48.2±2.90°C, respectively. The peak at 62.0°C appears only as a slight depression and almost not apparent. These two melting peaks correspond to the melting points of TO and BW albeit, a slight decrease in the melting point of BW. The total melting enthalpy for nanoformulation SDL3 was 11.8±2.5 J/g, being significantly lower than enthalpy values of SDL1 and SDL2 ($p \leq 0.01$ for pairwise comparisons). Nanoformulation SDL4 was prepared with

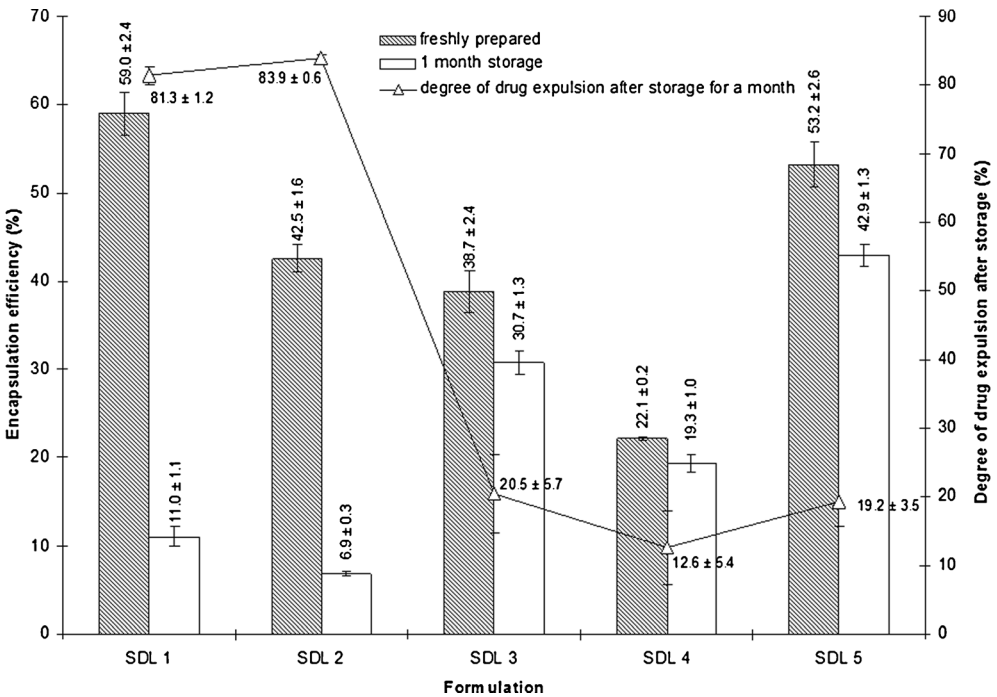

Fig. 3. Encapsulation efficiencies and degrees of AmB expulsion from freshly prepared lipid nanoparticles and after storage for 1 month (n=3)

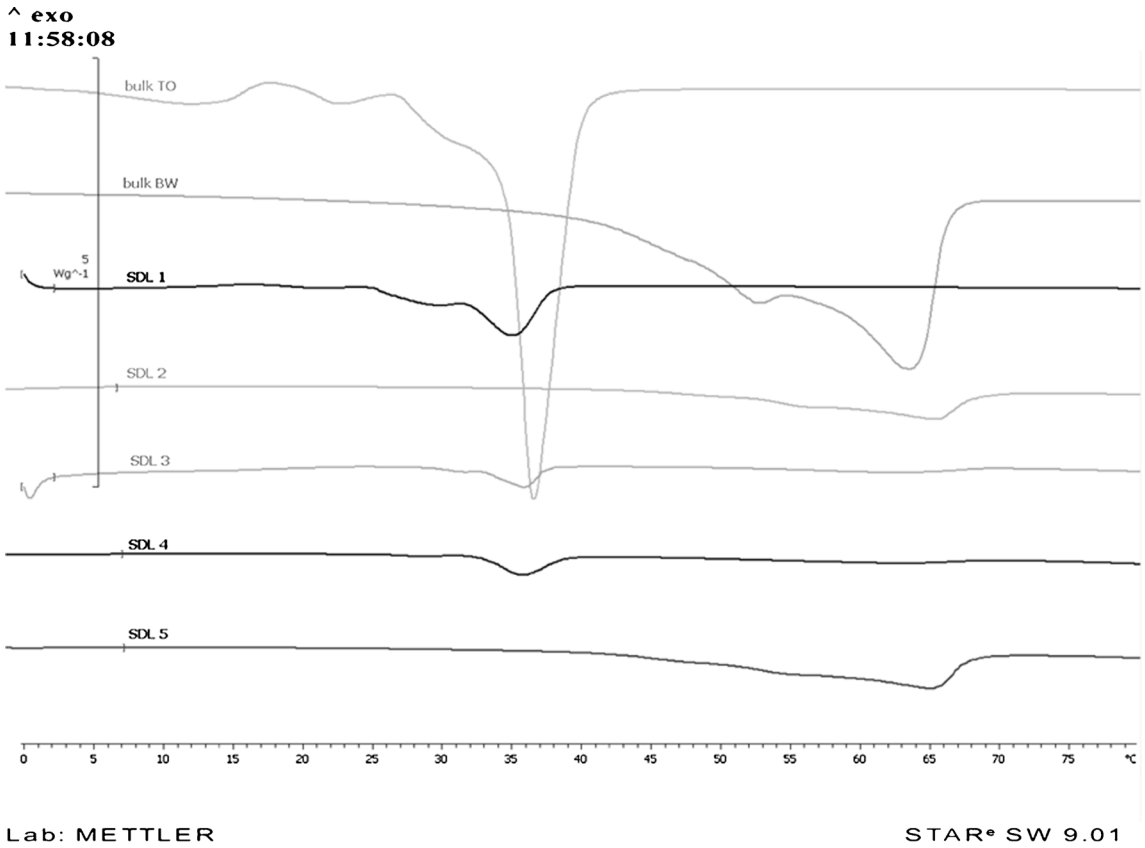

Fig. 4. Representative DSC thermograms of lipid nanoparticles

all three lipids (OA into TO and BW) in equal proportions, and we observed two melting peaks as in SDL3 at 35.6±0.09 (onset at 32.8±0.14°C) and 62.3±0.19°C (on set at 47.2±0.72°C), again representing melting peaks for TO and BW, respectively. In nanoformulation SDL4, where all three lipids are present in equal proportions, the lowest total melting enthalpy was observed at 8.0±0.49 J/g ($p \geq 0.05$). SDL5 which also contains the same types of lipid as in SDL2, but without lecithin, registered a peak minimum at 64.8±0.01°C which was insignificantly ($p \geq 0.05$) different from those in SDL2. The melting enthalpy of SDL5 was 31.3±1.28 J/g which is significantly higher ($p \leq 0.01$) than SDL2.

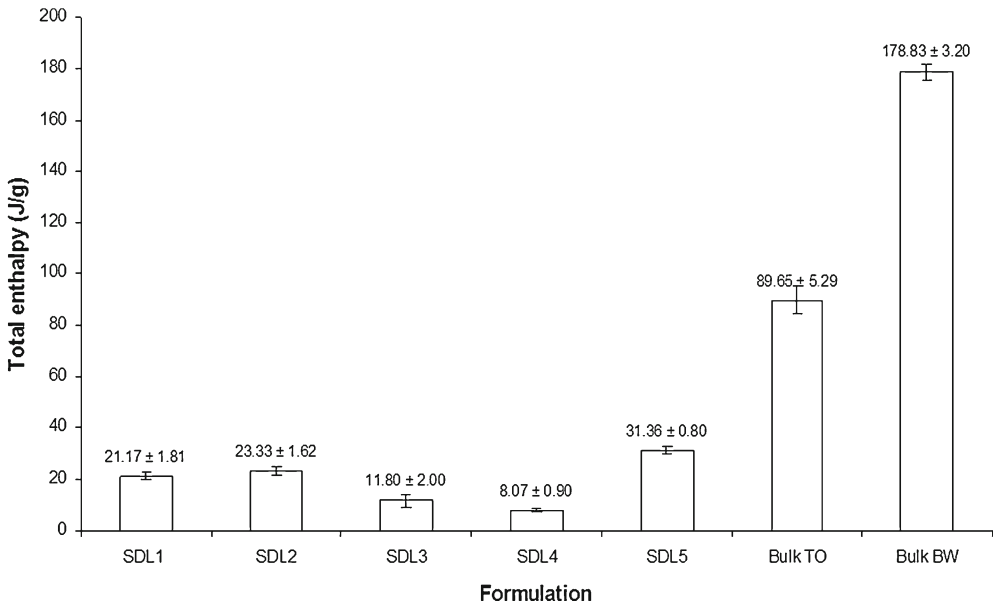

Fig. 5. Total melting enthalpy of lipid nanoparticles as calculated from DSC data ($n=3$)

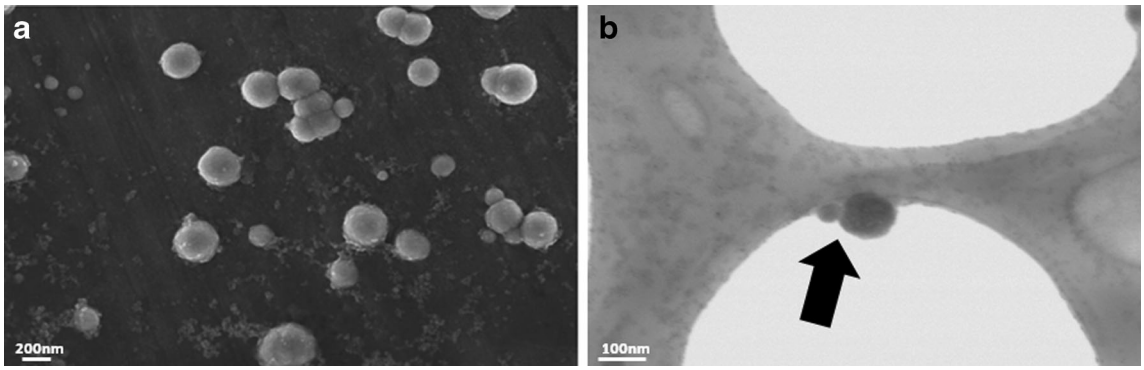

Fig. 6. FESEM (**a**) and STEM (**b**) images of nanoformulation

Expulsion of AmB During Storage

The calculated enthalpies in all the matrices prepared with lecithin (SDL1- 4) appear to mirror the degree of AmB expulsion after 1 month of storage displayed as displayed in Fig. 3. For example, whilst SDL4 had the lowest melting enthalpy, it also registered the lowest degree of AmB expulsion during storage. Conversely, SDL2, with a high enthalpy of 23.3±1.62 J/g, had the highest degree of AmB expulsion. SDL5 with BW as the lipid-forming matrix but formulated without lecithin, registered the highest total enthalpy at 31.3±0.8 J/g, significantly higher ($p \leq 0.01$) than the enthalpy from SDL2 (23.3± 1.62 J/g) also containing BW but without lecithin. Therefore, lecithin contributes increasing the enthalpy of the lipid matrices but its effect on degree of AmB expulsion is not as significant.

Crystals are associated with high melting enthalpies indicating that their lattices are ordered, and hence, more energy is required to dislocate the ordered arrangement. Such lattices also tend to expel any encapsulated drug expulsion during storage. Formulation SDL1 and SDL2 with total enthalpies measured as 21.1±1.81 and 23.3±1.62 J/g, respectively, subsequently, expelled 81.3 and 83.6% of AmB during storage. SDL1 and SDL2 were constructed with TO and BW, respectively, and as explained earlier, these lipids have the tendency of growing ordered lattices during storage. It appears that the BW forms a more ordered lattice within the nanoparticles compared with TO (based on enthalpy differences), attributable to alignment of the BW molecules into crystallites (19,24). The high degree of drug expulsion from SDL1 is most possibly due to the transformation of unstable polymorphic forms to stable β form within the crystal lattice of TO upon storage.

When both lipids were used in equal proportions by weight (SDL3), the nanoparticles registered an enthalpy of 11.8±2.0 J/g, expelling only 20.5% of AmB. At this ratio, the TO and BW lattice effects appear to dampen out because of the significantly lower enthalpy ($p \leq 0.01$) than the measured enthalpies when the lipids were used separately. A similar phenomenon has been reported previously by Attama *et al.* (25) where a lower total melting enthalpy was observed in SLN prepared with mixed lipids (TO and goat fat) compared with those prepared with single lipid. OA is a liquid at room temperature and when present within mixed BW/TO matrices (SDL 4), it contributes to the distortion of the ordered lattices contributed by BW and TO. Consequently, the measured enthalpy was the lowest, at 8.0±0.9 J/g and expelling only 12.6% of AmB. When BW was used alone without lecithin (SDL5), a higher enthalpy (31.3±0.8 J/g) was observed compared with when BW was used with lecithin. Therefore, lecithin can be said to impede the formation of ordered lattices. The high total melting enthalpy of SDL5 is possibly due to the formation of large particles during processing. The large particles were formed because of the absence of the surfactant lecithin. Larger particles would decrease the effective surface area of the lipid matrices that come in contact with the aqueous phase of the system thus minimizing the mass transfer of the encapsulated AmB. Thus, even though ordered lattices were formed in SDL5 and should ideally expel most of the AmB during storage, this effect was checked due to the larger-sized particles produced.

In summary, the lipid nanoparticles formulated with equal proportions of BW and TO (SDL3) appear to posses more optimal characteristics. Hence, FESEM and STEM characterizations were carried out on this formulation (SDL3) and compared with its dummy counterpart (SDL3-dummy) which was prepared in a similar manner apart from the absence of AmB.

FESEM and STEM Analyses

The morphological observation of the lipid nanoparticles under FESEM agreed with the PCS results, suggesting that the dispersed particles of the suspension exist as fairly discrete nanoparticles. FESEM analysis showed a generalized size of 250–300 nm (Fig. 6a). The STEM analysis indicates a uniform interior, which suggest that the nanoparticles exist as a matrix rather than a drug core shell (Fig. 6b).

CONCLUSION

We have successfully established the influence of TO, BW and OA on the physical properties of the formulated nanoparticles as well as the degree of Amb expulsion during 1 month storage. Whilst it was desirable to have imperfections imparted by OA within the solid lipid nanoparticles, a significantly lower %EE was manifested. When used as sole lipids, very high expulsion rates were observed for TO and BW. In combination, however, the expulsion of AmB was minimal. In view of the above data, we may conclude that solid lipid nanoparticles made from equal concentrations of TO and

BW produced the most desirable properties and worthy of further investigations.

REFERENCES

1. Lemke A, Kiderlen AF, Kayser O. Amphotericin B. Appl Microbiol Biotechnol. 2005;68:151–62.
2. Müller RH. Colloidal carriers for controlled drug delivery and targeting: modification, characterization and in vivo distribution. Boca Raton: CRC Press; 1991.
3. Kayser O, Olbrich C, Yardley V, Kiderlen AF, Croft SL. Formulation of amphotericin B as nanosuspension for oral administration. Int J Pharm. 2003;254:73–5.
4. Stuchlik M, Zak S. Lipid-based vehicle for oral drug delivery. Biomed Pap. 2001;145:17–26.
5. Attama AA, Müller-Goymann CC. A critical study of novel physically structured lipid matrices composed of a homolipid from *Capra hircus* and theobroma oil. Int J Pharm. 2006;322:67–78.
6. Mäder K, Mehnert W. Solid lipid nanoparticles—concepts, procedures, and physicochemical aspect. In: Nastruzzi C, editor. Lipospheres in drug targets and delivery: approaches, methods, and applications. Boca Raton: CRC Press; 2004. p. 1–22.
7. Fryer KPP. The material science of chocolate. MRS Bull. 2000;12:25–9.
8. Attama AA, Schicke BC, Müller-Goymann CC. Further characterization of theobroma oil-beeswax admixtures as lipid matrices for improved drug delivery systems. Eur J Pharm Biopharm. 2006;64:294–306.
9. Jenning V, Gohla S. Comparison of wax and glyceride solid lipid nanoparticles (SLN®). Int J Pharm. 2000;196:219–22.
10. Quintanar-Guerrero D, Fessi H, Allémann E, Doelker E. Influence of stabilizing agents and preparative variables on the formation of poly(D, L-lactic acid) nanoparticles by an emulsification-diffusion technique. Int J Pharm. 1996;143:133–41.
11. Rowe RC, Sheskey PJ, Owen SC. Handbook of pharmaceutical excipients. In: United Kingdom: American Pharmacists Association and Pharmaceutical Press; 2006. p. 850.
12. Landfeld A, Novotna P, Strohalm J, Houska M, Kyhos K. Viscosity of cocoa butter. Int J Food Prop. 2000;3:165–9.
13. Valeri D, Meirelles A. Viscosities of fatty acids, triglycerides, and their binary mixtures. J Am Oil Chem Soc. 1997;74:1221–6.
14. Komatsu H, Kitajima A, Okada S. Pharmaceutical characterization of commercially available intravenous fat emulsions: estimation of average particle size, size distribution and surface potential using photon correlation spectroscopy. Chem Pharm Bull (Tokyo). 1995;43:1412–5.
15. Levy MY, Schutze W, Fuhrer C, Benita S. Characterization of diazepam submicron emulsion interface: role of oleic acid. J Microencapsul. 1994;11:79–92.
16. Takamura A, Ishii F, Noro S, Tanifuji M, Nakajima S. Study of intravenous hyperalimentation: effect of selected amino acids on the stability of intravenous fat emulsions. J Pharm Sci. 1984;73:91–4.
17. Müller RH, Dobrucki R, Radomska A. Solid lipid nanoparticles as a new formulation with retinol. Acta Pol Pharm. 1999;56:117–20.
18. Jenning V, Gysler A, Schafer-Korting M, Gohla SH. Vitamin A loaded solid lipid nanoparticles for topical use: occlusive properties and drug targeting to the upper skin. Eur J Pharm Biopharm. 2000;49:211–8.
19. Schoening FRL. The X-ray diffraction pattern and deformation texture of beeswax. S Afr J Sci. 1980;76:262–5.
20. Basson I, Reynhardt EC. A new technique for determining the dielectric constants of a nematic liquid crystal. J Phys D Appl Phys. 1988;21:1421–8.
21. Hou D, Xie C, Huang K, Zhu C. The production and characteristics of solid lipid nanoparticles (SLNs). Biomaterials. 2003;24:1781–5.
22. Bernal JL, Jiménez JJ, del Nozal MJ, Toribio L, Martín MT. Physico-chemical parameters for the characterization of pure beeswax and detection of adulterations. Eur J Lipid Sci Tech. 2005;107:158–66.
23. Marangoni A, McGauley SE. Relationship between crystallization behavior and structure of cocoa butter. Cryst Growth Des. 2003;3:95–108.
24. Westesen K, Siekmann B, Koch MHJ. Investigations on the physical state of lipid nanoparticles by synchrotron radiation X-ray diffraction. Int J Pharm. 1993;93:189–99.
25. Attama AA, Schicke BC, Paepenmüller T, Müller-Goymann CC. Solid lipid nanodispersions containing mixed lipid core and a polar heterolipid: characterization. Eur J Pharm Biopharm. 2007;67:48–57.